

Uptake of inert microparticles in normal and immune deficient mice

S.H. Smyth^{a,*}, S. Feldhaus^b, U. Schumacher^b, K.E. Carr^c

^a *The Queen's University of Belfast, 71 University Road, Belfast BT7 1NN, UK*

^b *University Medical Centre, Hamburg Eppendorf, Germany*

^c *Department of Physiology, Anatomy and Genetics, University of Oxford, South Parks Road, Oxford, OX1 3QX, UK*

Received 21 March 2007; received in revised form 8 June 2007; accepted 13 June 2007

Available online 5 July 2007

Abstract

Intestinal microparticle uptake is important for drug delivery, environmental pollution and multiple organ dysfunction syndrome. This paper explores further whether uptake occurs at mucosa associated lymphoid tissue (MALT) via the microfold (M) cells of Peyer's patch domes or through villous epithelium. It does this by comparing the results of exposure of either severe combined immunodeficient (SCID) mice (lacking MALT) or normal BALBc mice, to oral gavage with 2 μm fluorescent latex microparticles. At 5 and 30 min after gavage, full circumference samples along the small intestine were processed for fluorescence microscopy and microparticle numbers were collected for surface and tissue sites. Uptake occurred in both BALBc and SCID mice within 5 min of particle administration and increased further in the following 25 min. In BALBc mice, almost all particles (96%) are in non-MALT sites in MALT circumference samples, with very few at the domes: uptake was also substantial in entirely villous samples. In SCID mice, particle numbers were only slightly lower than those of the BALBc mice, and occurred exclusively by the villous route. These findings confirm that the villous uptake route must be considered when assessing the extent of the dose delivered following pharmaceutical or toxicological oral exposure to microparticles.

© 2007 Elsevier B.V. All rights reserved.

Keywords: Small intestine; Latex microparticles; Uptake; Severe combined immunodeficiency (SCID); Mouse

1. Introduction

The key question being explored in this paper is whether microparticle uptake (Volkheimer et al., 1968) is able to take place in animals that entirely lack microfold (M)-cell containing Peyer's patches, since this would show that the presence of large quantities of mucosa associated lymphoid tissue (MALT), such as Peyer's patches, is not essential to the uptake process. The literature background to this question is that some groups report that uptake of microparticles through the small intestinal mucosal epithelium occurs at M cells of Peyer's patches (Ermak et al., 1995; Jepson et al., 1995; Thomas et al., 1996; Beier and Gebert, 1998). However, transepithelial passage through villous epithelium has been proposed as an alternative route (Desai et al., 1996; Hillyer and Albrecht, 2001). This difference of opinion may be due to the differences in experimental models, such as the administration of particles by single or multiple dosing,

the use of isolated intestinal loops as opposed to *in vivo in situ* models, or variations in the time-points chosen for sampling.

Other aspects of the methodology used are equally important. When total particle numbers are compared at Peyer's and non-Peyer's regions, uptake is reported for both (Limpanussorn et al., 1998; McClean et al., 1998), but the techniques used do not identify the precise route. Microscopic approaches are needed for this (McMinn et al., 1996). Our earlier work, using an *in vivo in situ* model, cryosections of full intestinal circumferences and fluorescence microscopy, showed that early uptake is predominantly villous: even in the region of Peyer's patches, the proportion of latex microspheres found at the follicle-associated epithelium (FAE) of the patches is very small, only in the order of 0.2% 30 min after gavage (Hodges et al., 1995), while the remaining 99.8% are seen elsewhere, with 73.7% associated with the enterocytes of the numerous villi around the rest of the patch-containing circumference. Direct comparison of entirely villous circumferences with those containing both villous and FAE regions shows no differences in particle numbers, whether this is estimated as particles per circumference or as particles per mm^2 intestinal section area, where the different areas taken up

* Corresponding author.

E-mail address: s.smyth@har.mrc.ac.uk (S.H. Smyth).

by Peyer's and non-Peyer's parts of the circumference are taken into account (Smyth et al., 2005). It is clear that terminology is important in defining where the uptake is taking place: this is set out in a later section of this paper.

The current paper directly addresses the hypothesis that if MALT containing Peyer's patches are the major uptake route, this will be absent or sharply reduced in animals lacking these organised MALT structures. The experimental model uses female severe combined immunodeficient (SCID) mice orally gavaged with 2 µm latex microparticles. The SCID data are compared with corresponding normal BALBc mouse particle numbers. The choice of species for this study is based on the fact that most work on immune deficient animals has been carried out on SCID mice and also that mouse Peyer's patches are known to contain considerable numbers of M cells (Sharma et al., 1996). The data on microparticle numbers for the two strains of mouse will be comparable with results already published for male mice (Doyle-McCullough et al., 2007) and also for rats, on which most of the *in vivo in situ* work already published has been based (Smyth et al., 2005).

There is already evidence that SCID mice are able to take up microorganisms, including bacteria (Ohsugi et al., 1996; Havell et al., 1999; Mutwiri et al., 2001) and parasites (Mead et al., 1991; Umemiya et al., 2005; Koudela et al., 1999), but it is also important to understand the mechanism of uptake of more inert microparticles, with respect to drug delivery systems (Eatock et al., 1999; Ravi Kumar, 2000) and the effect of pollutants (Bhattacharyya, 1983; Leazer et al., 2002).

The aim of the current paper is to explore microparticle uptake in animals lacking organised MALT such as Peyer's patches. The objectives are firstly, to confirm that *in vivo in situ* microparticle uptake in normal (BALBc) mice is mostly by the villous route at times soon after administration, even when regions containing MALT are studied; and secondly, to record the extent of uptake in animals lacking MALT and in particular M-cell containing Peyer's patches, thus testing the hypothesis that the villous uptake, which is so important in normal mouse intestine, occurs also in these immune deficient animals.

2. Materials and methods

2.1. Summary of protocols

Two groups of mice, normal and immune-deficient, were used to explore the effects on microparticle uptake of the absence of organised MALT. Procedures used include oral gavage with latex microparticles and preparation of intestinal samples for resin histology or for cryosectioning and subsequent fluorescence and confocal scanning laser microscopy. Sample collection was carried out through two separate experiments. To verify the effectiveness of the particle administration procedure for the experimental model used here, observations were made of the animals' response during particle administration and of the visibility of fluorescent particles in organs at post mortem or during sample preparation. Data collected included numbers of Peyer's patches in the BALBc mice and, for both strains, particle num-

bers in cross sections of small intestine, 5 and 30 min after gavage.

2.2. Animal groups and care

The experiments were carried out on two groups of young adult 9 week old, virgin female mice, namely BALBc ($n = 12$ experimental, 12 control) and SCID ($n = 12$ experimental, 12 control) in the Zentrum für Experimentelle Medizin, Institut für Anatomie II: Experimentelle Morphologie, Universitätsklinikum Hamburg-Eppendorf Hamburg, with the approval of the Behörde für Arbeit und Gesundheit (BAGS). The BALBc ($n = 24$ total) mice from the breeding program of the central animal facilities of the University Medical Centre, Hamburg Eppendorf, Germany were fed a maintenance diet-V1536-003 ssniff R/M-H (www.ssniff.de) and maintained under conventional conditions. The pathogen-free SCID ($n = 24$ total) mice from the same source were supplied with a sterile rodent diet as above and housed in sterile filter-top cages (autoclaved at 118 °C) on sterile Espe bedding (Abbed). Unlimited water was freely available to both strains.

2.3. Microparticles

The microparticles were plain (non-ionic) yellow-green fluorescent polystyrene latex microspheres (2.5% solids latex in water) with YG dye excitation maxima of 458 nm and emission maxima of 540 nm (Polysciences, Warrington, PA, USA). The particles were approximately 2 µm in diameter, although the exact dimensions varied slightly with batch. Particle dosage was a 0.1 ml suspension containing 5.68×10^8 particles.

2.4. Microparticle administration

Mice from each group were randomly assigned to receive either control or experimental treatment. Experimental animals ($n = 12$ per group) were orally gavaged with 0.1 ml particle suspension, using a 22 gauge gavage needle. Control mice ($n = 12$ per group) were gavaged with the same volume of sterile double-distilled water. After gavage, animals were replaced in their original cages with water freely available, but access to food denied.

2.5. Sample collection

Animals were killed either 5 min ($n = 6$ per group) or 30 min ($n = 6$ per group) later by an overdose of Sagatal¹ anaesthesia, delivered by intra-peritoneal injection. Appropriate measures were also taken to avoid cross-contamination from particle-fed to control-fed animals and samples. Immediately after death, animals were fixed by perfusion of 3% 0.1 M sodium cacodylate-buffered glutaraldehyde into the left ventricle: the small intestine was measured and divided into nine equal segments (Smyth et al., 2005).

¹ Sagatal, i.e. pentobarbitone sodium (60 mg/ml) available from Rhone Merieux Ltd., Spire Green Centre, Harlow, UK.

2.6. Preparation of resin sections for histology

For resin histology, full circumference portions from the samples were washed in 0.1 M sodium cacodylate buffer, dehydrated in ethanol, through 50%, 70%, 90% and 100% solutions and then embedded in epoxy resin. Sections approximately 2 μm thick were cut on a Reichert-Jung Ultracut E microtome, dried and stained with toluidine blue and then examined and photographed using standard light microscopy techniques.

2.7. Preparation of cryosections

Samples of full circumference rings approximately 5 mm in length, including MALT (a Peyer's patch) if present, were also prepared from all nine segments as previously published (Smyth et al., 2005). They were washed with three changes of 0.1 M sodium cacodylate buffer, blotted dry, frozen in liquid nitrogen-cooled isopentane and cut using a Leica CM1900 cryostat to produce 14 μm -thick sections. These were stained with 1 $\mu\text{g}/\text{ml}$ propidium iodide for 30 min and washed with buffer to remove excess stain. They were then mounted on APES-coated (3-aminopropyltriethoxysilane) slides, using Gelvatol mounting medium (Cairn Chemicals Ltd., Chesham, Buckinghamshire, UK). At least three sections per sample were analysed with fluorescence microscopy.

The presence of organised MALT such as Peyer's patches was recorded.

2.8. Particle counting

The segments were designated as either 'MALT' or 'entirely villous' (Fig. 1). If a segment contained one Peyer's patch or more, a full circumference sample was prepared from one of these. If a segment had no Peyer's patches and was entirely villous, a full circumference sample was selected at random for study.

Particle numbers were counted with a Leitz (Leica) Diaplan fluorescence microscope using fluorescein filter settings, with maximum excitation of 445 nm and maximum emission of 550 nm. The particles were allocated to several sites, with the names of these differing slightly according to whether the segment was MALT or entirely villous.

For MALT segments, the regions and sites were: 'luminal' (luminal, inter-villous); 'mucosal surface' (surface enterocytes, surface goblet cells); 'villous' (villous enterocytes, goblet cells, lamina propria); 'cryptal' (cryptal epithelium, pericryptal stroma); 'dome' (follicle-associated epithelium where present, or lymphocyte-associated epithelium, lymphoid tissue); and 'deeper tissues' (submucosa, blood vessels, muscularis externa and serosa).

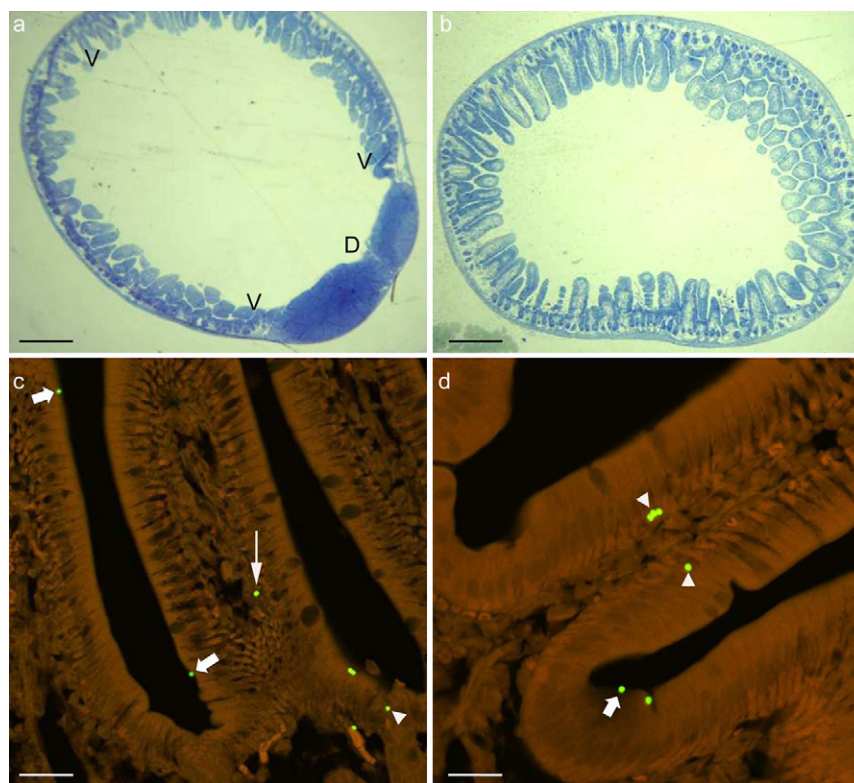


Fig. 1. Terminology and particle visualization. Resin histology (a) and (b) and confocal scanning laser microscopy (c) and (d) of mouse small intestine. The resin histology sections illustrate the terminology used. MALT section (a) shows domes covered with FAE (D) and villi (V), the latter taking up most of the circumference. Such segments are only found in BALBc mice: this image has been digitally cleaned to illustrate better the dome regions. Entirely villous segments (b), shown here from a SCID mouse, are also found in BALBc mice, in the segments lacking FAE domes. Confocal scanning laser microscopy (c) and (d) of cryosections stained with propidium iodide reveals particles in BALBc (c) and SCID (d) mice, on the mucosal surface (thick arrows) and within enterocytes (arrow heads); the thin arrow shows a particle which is probably within the villous stromal compartment. Bars equal approximately (a) 1.0 mm; (b) 1.3 mm; (c) 18.0 μm ; (d) 12.9 μm .

For entirely villous segments, the sites included only the luminal, villous, cryptal and deeper tissues groups of possible locations for the particles.

For comparison of uptake through a possible M cell/Peyer's route as opposed to a villous route, the particle numbers in MALT segments and entirely villous segments were compared animal by animal: in the MALT segments, the particles were designated as 'dome' or 'villous': particles in submucosal and deeper layers were not included.

The fact that particles were in and not on sections was confirmed in a proportion of sections using a Bio-Rad MRC 600 laser scanning confocal microscope with argon laser, operated in dual-channel mode, using serial optical slicing: some images were also recorded using a Zeiss LSM510 META detector system.

2.9. Calculation of tissue particle numbers/tissue uptake

For this, numbers were added for all but luminal and mucosal surface regions. An estimate of total tissue particle numbers was obtained by calculating the sum of the mean values for all nine segments. The percentage of total administered particles was calculated using the following equation:

$$\text{percentage administered dose} = \left(\frac{(\text{tissue uptake}/\text{length sampled } (14 \times 9 \mu\text{m})) \times \text{intestinal length}}{\text{total particles gavaged}} \right) \times 100$$

Particle numbers were compared across the groups for total particle numbers and for proximodistal distribution: statistical analysis was carried out on these data. However, for the display of uptake as 'dome' or 'villous', the separation of the segments into MALT and entirely villous subgroups meant that not all 'n' numbers were large enough to permit statistical analysis.

2.10. Data analysis

All analysis was done blind on coded specimens and the assessment of particle counts in small intestinal cryosections was carried out by the same observer. Data sets were analysed, where appropriate, using the Kruskal–Wallis and Mann–Whitney *U* non-parametric statistical tests with significance reported at $p < 0.05$.

3. Results

3.1. Terminology for location of uptake

This has been described in Section 2. In summary, the term segment is used for one of the nine equal parts of the small intestine, the term sample for a full circumference piece cut from a fixed segment, the term section for a $14 \mu\text{m}$ cryosection or resin section prepared from a sample and the term site for one of the cell or tissue locations within the intestinal tissue in a section. As above, the term MALT segment is used when a full

circumference sample from it contains a dome and surrounding villi: the subdivisions here are MALT (dome) and MALT (villous). The domes take up a very small part of the circumference (Fig. 1a). The other segments are described as entirely villous.

3.2. Confirmation of success of gavage

The effectiveness of the gavage procedure for the experimental animal model used here was confirmed by the observation at dissection, through the gastrointestinal wall, of yellow fluorescence related to the presence of particles and by the presence of particles in the lumen of the small intestine. Particles were not found in any small intestinal sections of animals gavaged with distilled water.

3.3. Immune status

A majority, 65.7%, of the BALBc full circumference samples were from MALT segments, but none from the SCID mice groups contained any organised MALT (Fig. 1b). Only one example of disorganised lymphoid tissue was seen in a SCID mouse, but this could not be regarded as a structurally complete Peyer's patch.

Particles can be identified associated with various intestinal sites in both groups of mice (Fig. 1c and d). Total tissue uptake was 0.04% (S.E. ± 0.004) of the administered dose at 5 min for BALBc mice. This increased significantly to 0.27% (S.E. ± 0.02) at 30 min. The same pattern of significant increase was seen for the SCID groups, with 0.01% (S.E. ± 0.003) and 0.21% (S.E. ± 0.03) the levels at 5 and 30 min, respectively. The two groups differed in total uptake only at 5 min, when BALBc values were nearly seven times higher (Table 1, Fig. 2).

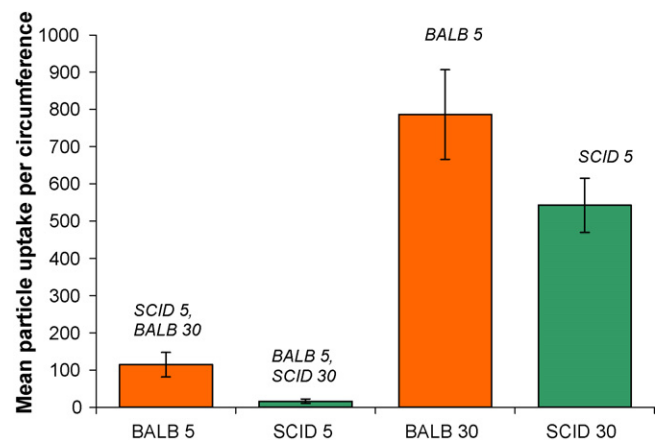


Fig. 2. Mean particle uptake. Mean tissue uptake of latex particles for small intestinal segments 1–9 per $14 \mu\text{m}^2$ circumference sections, at 5 and 30 min after administration, in both virgin female BALBc and SCID mice ($n=6$ per group). Bars indicate standard error of the mean. Above each column is a note of any other groups (in italics) that differ from it significantly ($p \leq 0.05$) following comparison with both Kruskal–Wallis and Mann–Whitney *U* non-parametric statistical tests (e.g. for column 1, there was a significant difference when mean particle uptake per circumference in the BALBc 5 min group was compared with that in the SCID 5 min group and in the BALBc 30 min group).

Table 1
Mean tissue distribution of latex particles 5 min after administration

Tissue site/region	Small intestinal segments 1–9 (1st value is from BALBc group/2nd value is from SCID group)									Total 1–9
	1	2	3	4	5	6	7	8	9	
Lumen, in the centre	7/3	5/<1	1/0			No particles in either group				12/3
Intervillous, between villi	52/19	22/<1	<1/0			No particles in either group				74/19
<i>Luminal (subtotal)</i>										(86/22)
Enterocyte surface, adsorbed	95/16	38/<1	86/0			No particles in either group				135/16
Goblet cell surface, adsorbed	12/5	5/0	<1/0			No particles in either group				17/5
<i>Mucosal surface (subtotal)</i>										(152/21)
Enterocyte	35/8	12/<1	<1/0			No particles in either group				48/8
Goblet cell	4/1	1/0	<1/0			No particles in either group				5/1
Lamina propria	20/5	14/<1	<1/0			No particles in either group				34/5
<i>Villous regions (subtotal)</i>										(87/14)
Cryptal epithelium	2/2	1/0	<1/0			No particles in either group				3/2
Pericryptal stroma	4/1	5/<1	<1/0	<1/0	<1/0	No particles in either group				10/1
<i>Cryptal regions (subtotal)</i>										(13/3)
Dome epithelium	0/0	2/0				No particles in either group				2/0
Underlying lymphoid tissue if present	0/0	2/0				No particles in either group				2/0
<i>MALT (subtotal)</i>										(4/0)
Submucosa	4/1	2/0	<1/0	0/0	0/0	0/0	<1/0	0/0	0/0	7/1
Blood vessels	2/0	<1/0				No particles in either group				2/0
Muscularis and serosa	2/<1	<1/0				No particles in either group				2/<1
<i>Deeper tissues (subtotal)</i>										(11/1)
<i>Total tissue uptake (Villous, cryptal, MALT + deeper regions)</i>										115/18

Data are mean numbers of particles per $14 \mu\text{m}^2$ circumference section for virgin female BALBc and SCID mouse small intestinal segments 1–9 ($n = 6$ per group). MALT is either Peyer's patches (BALBc groups) or lymphocyte-associated epithelium (SCID groups), if present. The ratio of luminal/mucosal surface particle numbers for mean values for segments 1–9 for BALBc mice is 1.76 and for SCIDs is 0.95. Corresponding ratios for mucosal surface/total tissue uptake are 0.76 for BALBc mice and 0.86 for SCIDs.

These differences are related to the details of proximodistal transit (Fig. 3), the extent of uptake and the specific sites involved. However, the ratios of overall particle numbers for luminal/mucosal surface and mucosal surface/total tissue uptake were similar across the strains (Tables 1 and 2).

In both strains 5 min after gavage, luminal particles were concentrated proximally, but BALBc mice had substantial numbers (≥ 10 per circumference) as far distally as segment 2, one segment more distal than the SCID animals (Table 1): in addition, particles at this level were also found in the mucosal surface region as far as segment 3 in the BALBc group. This was reflected in greater BALBc tissue particle numbers in these proximal parts of the small intestine and larger numbers of particles which had moved through the epithelial layer into the stroma, blood vessels and deeper layers.

By 30 min after particle administration, the equal uptake in the two strains reflected increases in the intervening 25 min by factors of approximately 7 for the BALBc groups and 30 for the SCID groups (Table 2, Fig. 2). The higher, sharper luminal

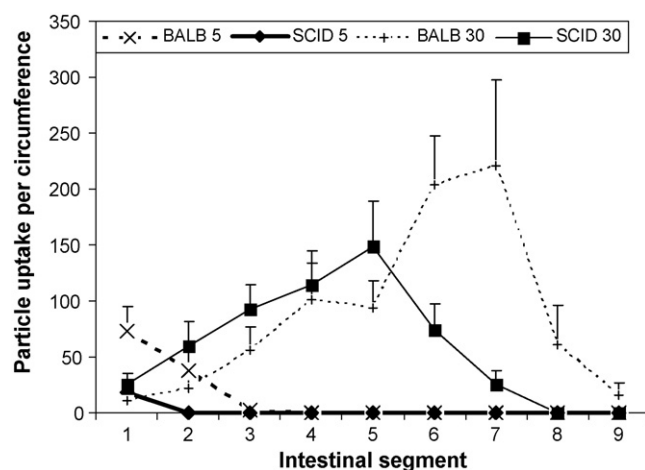


Fig. 3. Proximodistal particle distribution. Mean tissue distribution of latex particles per $14 \mu\text{m}^2$ circumference samples in small intestinal sections 1–9 for time-points 5 and 30 min after administration for virgin female BALBc and SCID mice ($n = 6$ per group). Standard errors are shown above each point.

Table 2
Mean tissue distribution of latex particles 30 min after administration

Tissue site/region	Small intestinal segments 1–9 (1st value is from BALBc group/2nd value is from SCID group)									Total 1–9
	1	2	3	4	5	6	7	8	9	
Lumen, in the center	3/6	87/15	46/4	5/3	25/15	21/7	18/17	37/<1	<1/0	242/66
Intervillous, between villi	9/32	15/40	41/55	99/58	89/171	277/185	743/28	350/<1	92/<1	1712/570
<i>Luminal (subtotal)</i>										1954/636
Enterocyte surface, adsorbed	9/28	24/44	42/78	96/93	113/123	362/167	506/49	187/<1	77/<1	1415/584
Goblet cell surface, adsorbed	1/4	4/7	7/10	15/12	18/21	36/22	68/7	16/0	15/<1	180/83
<i>Mucosal surface (subtotal)</i>										1595/667
Enterocyte	6/17	10/25	26/41	53/51	42/64	61/26	99/6	32/0	9/<1	337/231
Goblet cell	<1/2	1/4	3/6	7/9	8/13	15/7	19/2	10/0	2/<1	65/42
Lamina propria	2/4	6/18	14/28	19/30	22/33	65/16	56/5	12/<1	4/<1	200/133
<i>Villous regions (subtotal)</i>										602/406
Cryptal epithelium	<1/1	<1/2	1/4	4/5	4/4	8/4	12/2	<1/0	<1/0	31/24
Pericryptal stroma	<1/1	2/3	4/5	8/7	5/16	18/4	18/4	3/0	<1/<1	59/40
<i>Cryptal regions (subtotal)</i>										90/64
Dome epithelium	0/0	<1/0	2/0	2/0	<1/0	2/<1	2/0	<1/0	<1/0	9/<1
Underlying lymphoid tissue if present	0/0	<1/0	3/0	3/0	<1/0	4/1	4/0	1/0	<1/0	17/1
<i>MALT (subtotal)</i>										26/1
Submucosa	1/<1	1/3	4/5	4/7	8/13	27/12	7/4	1/0	<1/0	55/46
Blood vessels	<1/<1	0/3	<1/1	0/1	<1/4	2/<1	<1/<1	<1/0	0/0	3/10
Muscularis and serosa	<1/<1	<1/2	<1/2	<1/4	2/3	2/3	3/2	<1/0	0/0	9/15
<i>Deeper tissues (subtotal)</i>										67/71
<i>Total tissue uptake (Villous, cryptal, MALT + deeper regions)</i>										785/542

Data are mean numbers of particles per 14 μm^2 circumference section for virgin female BALBc and SCID mouse small intestinal segments 1–9 ($n = 6$ per group). MALT is either Peyer's patches (BALBc groups) or lymphocyte-associated epithelium (SCID groups), if present. The ratio of luminal/mucosal surface particle numbers for mean values for segments 1–9 for BALBc mice is 0.82 and for SCIDs is 1.05. Corresponding ratios for mucosal surface/total tissue uptake are 0.49 for BALBc mice and 0.81 for SCIDs.

peak at segment 7 in BALBc groups (Table 2) contrasted with a flatter, more proximal distribution in the SCIDs: this contributed to the significantly larger number of luminal particles overall in BALBc groups. However, this was not reflected in overall increases in surface or tissue particles: although the segment 7 peak was present, this was compensated for by lower particle numbers elsewhere.

3.4. MALT versus villous uptake

In BALBc mice, 3.5% of the total particle numbers were found at the MALT domes, while the corresponding figure for SCIDs was zero, since no organised MALT was present. In the 30 min group, a similar proportion (3.3%) of the particles were located at the MALT domes in the BALBc groups but there were no MALT-associated particles in SCID mice.

The amount of MALT in segments 1 through 9 increased distally (Table 3). When the mucosal epithelial and stromal particle numbers in MALT circumferences for BALBc mice were divided into dome and villous sites, it can be seen (Fig. 4) that almost all the uptake is villous.

3.5. Onward movement of particles

Although the total uptake was similar in villous epithelial and stromal sites, 30 min after gavage, the BALBc groups had more particles in the FAE and underlying lymphatic tissue, while the

Table 3
Proximodistal distribution of MALT domes

Segment	Number of animals with MALT domes	
	BALB 5 min	BALB 30 min
1	3	3
2	4	4
3	2	5
4	3	4
5	1	3
6	6	5
7	4	3
8	5	5
9	5	6

Data are number of segments containing MALT domes at the 5 and 30 min time point in BALBc mice: $n = 6$ per point. No organised MALT was found in the SCID mice.

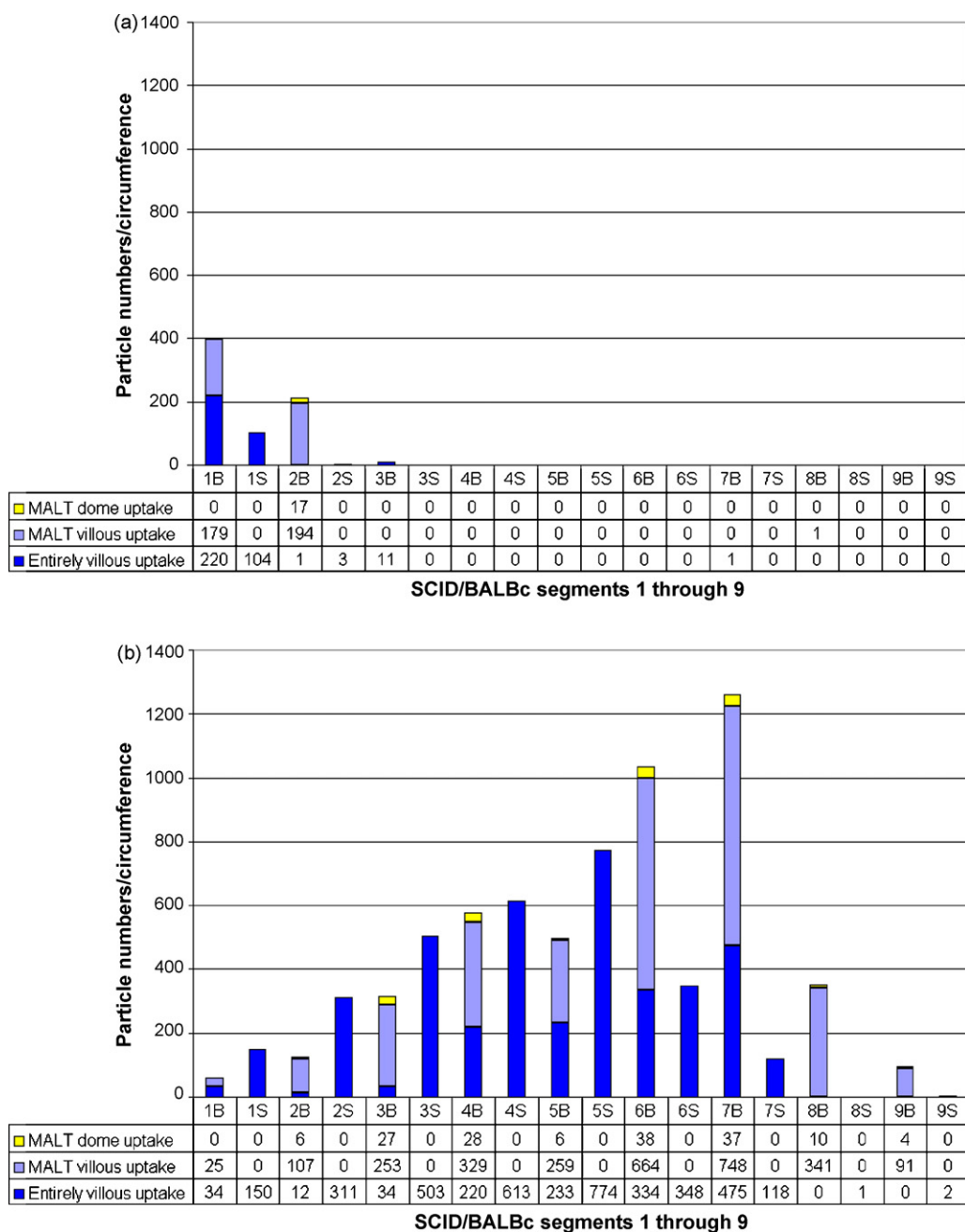


Fig. 4. Villous and dome uptake. For distribution of particle uptake, particle location is in the mucosa of either MALT dome (yellow), MALT villous sites (pale blue) or entirely villous segments (dark blue) for 5 min (a) and 30 min (b). For the calculations, the particles found in submucosal and deeper layers were excluded, to ensure that the only particles included are those associated with dome or villous epithelium or the mucosal stroma deep to it. The BALBc data are labelled 1B etc and the SCID data 1S etc, with the numbers relating to the proximodistal segment involved. The numbers below each histogram bar are the values summed for the six animals, displayed according to where they were found: the n values for MALT distribution in BALBc mice are in Table 3. At both time points almost all uptake is villous in BALBc mice, with very few particles in MALT domes: all uptake is villous in SCID mice. (For interpretation of the references to colour in this figure legend, the reader is referred to the web version of the article.)

SCID animals had significantly more particles in blood vessels, although the numbers were small (Table 2).

4. Discussion

The aim of this paper is to compare microparticle uptake in immunologically intact MALT-containing BALBc mice with that in severe combined immunodeficient (SCID) mice, where

organised MALT is almost non-existent. The discussion begins by considering some important details of the experimental model, including the method of calculation of particle uptake. Intraluminal transit and potential barriers to uptake are then examined, followed by consideration of the predominant villous route of uptake and the potential role of the epithelial tight junctions. Finally, the pathways for the onward movement of particles are reviewed.

The experimental model directly compares the two strains of mice. Morphological examination confirmed that the SCID mice had normal villous morphology (Hoshi et al., 2001) but greatly reduced MALT (Furrie et al., 1994). Developmental failure of the immune system may not always be quite complete, allowing for the possibility of the presence of cryptopatches, isolated lymphoid follicles or lymphocyte-filled villi (Moghaddami et al., 1998; Hitosumatsu et al., 2005). However, in the present experiments, only a single example of disorganised lymphoid tissue was identified in a SCID mouse: uptake of particles through such regions can therefore be discounted.

Successful gavage into the gastrointestinal lumen is initially confirmed by observation of animal behaviour (Smyth et al., 2005; Doyle-McCullough et al., 2007). The microparticles are non-ionic, non-toxic and their fluorescent colouring can be seen at dissection through the gastrointestinal wall, confirming successful gavage: they can also be quantified in sections by fluorescence microscopy. The intra-peritoneal anaesthetic overdose used to kill the mice could affect gastrointestinal motility (Sababi and Bengtsson, 2001) or transit (Freye et al., 1998). Uptake of microparticles has been reported from 10 min (Jenkins et al., 1994) to 2 days (Jani et al., 1992): the 'early' time points of 5 and 30 min used here allowed observation of the first microparticles crossing the small intestinal barrier. The times were chosen with reference to earlier work, showing that intestinal tissue particle numbers for a comparable rat *in vivo in situ* model were substantially higher at these early time points than at later times, such as between 2 and 24 h after particle administration (Hodges et al., 1995; Hazzard et al., 1996). It is also important to recall that the use of microscopic techniques allows more accurate identification of particle numbers taken into the tissue, without artefactual inclusion of those that are merely attached to the mucosal surface (McMinn et al., 1996).

When total uptake per administered dose is used to estimate particle numbers 30 min after gavage, the figure obtained from the present study of 0.27% for female BALBc mice compares well with previous reports of 0.13% for female rats (Smyth et al., 2005), and 0.32% and 0.13% for male mice and rats respectively (not significantly different; Doyle-McCullough et al., 2007). When mean numbers per circumference are compared, the female rat levels appear different from those in mice, while for the males this is not the case. However, the differences relate only to the relative levels of significance. The total uptake figures for the BALBc mouse model 30 min after administration are also consistent with published data, from 0.01 to 0.37% (LeFevre et al., 1985; Ebel, 1990; Jenkins et al., 1994). Although these microparticle numbers represent only a small fraction of the dose administered, it has implications for drug and vaccine administration and for toxicology (Florence and Hussain, 2001).

Before addressing the experimental data on tissue particle numbers, intra-luminal transit must first be considered, since intestinal uptake will only occur once this is achieved. In the female, such as the model used here, stomach emptying may be influenced by bolus characteristics, stress, stage of oestrous cycle and age (Naliboff et al., 2004; Gonenne et al., 2006). Liquid doses should pass quickly through the pyloric sphincter to the small intestine (Fich et al., 1990) and this was seen for the

current model of latex particles suspended in distilled water at 5 min in all animals, confirming previous reports of rapid delivery (Jenkins et al., 1994; Hazzard et al., 1996). Luminal and surface particles were found more distally and in higher numbers in the BALBc group than in the SCIDs, where uptake must be affected by this slower transit: this is reflected in greater tissue particle numbers distally in the BALBc mice. Once transit mechanisms have delivered the particles to the intestinal lumen, their uptake through the epithelium must be preceded by a journey through its mucus covering, known to be open to variation (Sharma et al., 1995; Sharma and Schumacher, 2001). The next barrier is the glycocalyx, which has been reported to prevent uptake of 1 μm diameter microparticles (Frey et al., 1996).

It is clear from the data presented here that uptake does occur in SCID intestine, thus addressing the aim of the work. This confirms for inert particles what has already been reported for organisms in primary or secondary uptake (Ohsugi et al., 1996; Havell et al., 1999), although the mechanism may be different: comparison of levels of uptake is also difficult, since recording the presence of pathogens either involves counting cultured organisms, as above, or qualitative descriptions of morphological changes (Autenrieth and Firsching, 1996; Umemiya et al., 2005), as opposed to direct observation, in the case of latex particles in small intestinal tissue.

This study confirms reports that uptake in an *in vivo in situ* model is predominantly villous, as described for rats (Hodges et al., 1995; Doyle-McCullough et al., 2007). The fact that 96% of the particle numbers are at non-dome sites in BALBc mice fits well with these earlier figures: the first objective of this study has therefore been addressed.

The absence of MALT, however, by no means stops microparticle uptake. Although the figure for percentage uptake at 5 min for SCID small intestinal tissue is significantly lower than that for the BALBc strain, both values are small. Similar uptake levels in the two strains 25 min later imply that the SCID group rate has been higher in the intervening period. These findings address the second objective of the work and are in line with the report that *Listeria* infection, previously thought to be mediated only through Peyer's patches, was found in SCID mice (Havell et al., 1999) and therefore related to uptake mediated by enterocytes.

It could be argued for the BALBc mice that microparticles might enter through the MALT route before moving through the connective tissue and upwards into nearby villi and that even the 5 min time point used here is too late to observe the 'M cell phase' of this process. However, there are three flaws in this argument. Firstly, large numbers of particles are found in the villous epithelium itself instead of just in the stroma, as would be the case if they were coming from the Peyer's patches; secondly, microparticle uptake continues through the villous route even in the SCID animals with no organised MALT; and finally, when sampling is done even earlier, two minutes after gavage, uptake at villous enterocytes still occurs to a greater extent than at MALT (Campbell et al., 2000).

The pathway of trans-epithelial uptake is still open to debate. For the villous route (Desai et al., 1996; McClean et al., 1998; Hillyer and Albrecht, 2001), uptake *in vivo* may be both intra- and intercellular, via enterocytes. The intracellular (para-

cellular) mechanism is observed for the endocytotic uptake of nanoparticles (Fattal et al., 1998). The paracellular route involves movement through tight junctions (TJs), which perform gate and barrier functions between the apical parts of adjacent cells and can be manipulated to allow pharmaceutical agents through the epithelial barrier (Gonzalez-Mariscal et al., 2005). The knockdown of JAM1, a component of TJs, increases paracellular permeability in epithelial monolayers (Mandell et al., 2005) and this protein is needed to control the paracellular migration of monocytes during immune reactions (Martin-Padura et al., 1998). The possible involvement of TJs in uptake in the *in vivo in situ* model has recently been simulated *in vitro* (Moyes et al., 2007), but the mechanism for microparticle uptake by the paracellular route is not yet clearly understood.

Finally, little can be deduced from the current data about the onward movement of particles after their initial uptake through the small intestinal wall. However, the observation that the SCID mechanism led to more particles in intestinal blood vessels than BALBc groups thirty minutes after gavage suggests that the former group might rely more on a blood route of particle onward movement, since their lymphoid involvement is reduced. This correlates with reports of hepatic disease in SCID mice that have taken up pathogenic organisms such as *Listeria*, *Cryptosporidium* and murine rotavirus (Riepenhoff-Talty et al., 1989; Mead et al., 1991; Havell et al., 1999), implicating a blood/portal vein/liver route from the small intestinal wall. Also relevant is the likely involvement of macrophages in the removal of *E. coli* after intragastric delivery (Ohsugi et al., 1996). This implies that following the TJ-moderated paracellular path proposed above, there may be microparticle translocation via a route involving macrophages, intestinal veins and the portal vein in the immune-deficient mice, whereas the lacteal, thoracic duct, lymph node route will also be important in normal rodents.

The current data therefore do not address the important question of how to increase uptake into Peyer's patches in order to increase the immunological response to orally administered vaccines. They do however complete the series of experiments underlining the fact that uptake apparently taking place at the Peyer's containing samples appears in an *in vivo in situ* model occur almost entirely at the adjacent villi and not through the FAE of the dome of the patch. This highlights the fact that the results are of importance in the context of past data on the routes of uptake. However, the results also point to the tight junctions between the villous epithelial cells as a possible route of entry and therefore draw attention to the importance of the literature on the role of these junctions in drug delivery across epithelial layers such as are seen in the small intestine (Gonzalez-Mariscal et al., 2005).

In conclusion, the data presented confirm that microparticle uptake apparently occurring at Peyer's patches in normal BALBc mice is almost entirely due to passage through villous epithelium, whether near or distant from MALT. They also show that, despite the absence of organised MALT, uptake of inert particles occurs in immune-deficient mice. This may imply that the previously reported uptake of biologically active entities is not

wholly dependent on an invasive process initiated by the microorganisms, but may also involve the trans-epithelial mechanism used by the latex microparticles.

Acknowledgements

We are grateful to members of the technical staff for assistance; to Mr Ken Lee and also to staff at the Oxford Brookes University for help with the confocal scanning laser microscopy; to Dr Chris Patterson and Mr David Papworth for statistical advice; to Ms Siobhan Moyes and Mr Colin Beesley for help with the data presentation; and to Professor John Morris and Ms Moyes for comments on the manuscript.

References

- Autenrieth, I.B., Firsching, R., 1996. Penetration of M cells and destruction of Peyer's patches by *Yersinia enterocolitica*: an ultrastructural and histological study. *J. Med. Microbiol.* 44, 285–294.
- Bhattacharyya, M.H., 1983. Bioavailability of orally administered cadmium and lead to the mother, fetus, and neonate during pregnancy and lactation: an overview. *Sci. Total Environ.* 28, 327–342.
- Beier, R., Gebert, A., 1998. Kinetics of particle uptake in the domes of Peyer's patches. *Am. J. Physiol.* 275, G130–G137.
- Campbell, M., Smyth, S.H., Hazzard, R.A., Carr, K.E., 2000. Influence of latex microparticle size on initial uptake in the rat small intestine. *J. Anat.* 197, 328.
- Desai, M.P., Labhasetwar, V., Amidon, G.L., Levy, R.J., 1996. Gastrointestinal uptake of biodegradable microparticles: effect of particle size. *Pharm. Res.* 13, 1838–1845.
- Doyle-McCullough, M., Smyth, S.H., Moyes, S.M., Carr, K.E., 2007. Factors influencing intestinal microparticle uptake in vivo. *Int. J. Pharm.* 335, 79–89.
- Eatock, M., Church, N., Harris, R., Angerson, W., McArdle, C., French, R., Twelves, C., 1999. Activity of doxorubicin covalently bound to a novel human serum albumin microcapsule. *Invest. New Drugs* 17, 111–120.
- Ebel, J.P., 1990. A method for quantifying particle absorption from the small intestine of the mouse. *Pharm. Res.* 7, 848–851.
- Ermak, T.H., Dougherty, E.P., Bhagat, H.R., Kabok, Z., Pappo, J., 1995. Uptake and transport of copolymer biodegradable microspheres by rabbit Peyer's patch M cells. *Cell Tissue Res.* 279, 433–436.
- Fattal, E., Vauthier, C., Aynie, I., Nakada, Y., Lambert, G., Malvy, C., Couvreur, P., 1998. Biodegradable polyallylcyanoacrylate nanoparticles for the delivery of oligonucleotides. *J. Control. Rel.* 53, 137–143.
- Fich, A., Neri, M., Camilleri, M., Kelly, K.A., Phillips, S.F., 1990. Stasis syndromes following gastric surgery: clinical and motility features of 60 symptomatic patients. *J. Clin. Gastroenterol.* 12, 505–512.
- Florence, A.T., Hussain, N., 2001. Transcytosis of nanoparticle and dendrimer delivery systems: evolving vistas. *Adv. Drug Deliv. Rev.* 50, S69–S89.
- Frey, A., Giannasca, K.T., Weltzin, R., Giannasca, P.J., Reggio, H., Lencer, W.I., Neutra, M.R., 1996. Role of the glycocalyx in regulating access of microparticles to apical plasma membranes of intestinal epithelial cells: implications for microbial attachment and oral vaccine targeting. *J. Exp. Med.* 184, 1045–1059.
- Freye, E., Sundermann, S., Wilder-Smith, O.H., 1998. No inhibition of gastro-intestinal propulsion after propofol- or propofol/ketamine-N₂O/O₂ anaesthesia. A comparison of gastro-caecal transit after isoflurane anaesthesia. *Acta Anaesthesiol. Scand.* 42, 664–669.
- Furrie, E., Turner, M.W., Strobel, S., 1994. Failure of SCID mice to generate an oral tolerogen after a feed of ovalbumin: a role for a functioning gut-associated lymphoid system. *Immunology* 83, 562–567.
- Gonenne, J., Esfandyari, T., Camilleri, M., Burton, D.D., Stephens, D.A., Baxter, K.L., Zinsmeister, A.R., Bharucha, A.E., 2006. Effect of female sex hormone supplementation and withdrawal on gastrointestinal and colonic transit in postmenopausal women. *Neurogastroenterol. Motil.* 18, 911–918.

- Gonzalez-Mariscal, L., Nava, P., Hernandez, S., 2005. Critical role of tight junctions in drug delivery across epithelial and endothelial cell layers. *J. Membr. Biol.* 207, 55–68.
- Havell, E.A., Beretich Jr., G.R., Carter, P.B., 1999. The mucosal phase of *Listeria* infection. *Immunobiology* 201, 164–177.
- Hazzard, R.A., Hodges, G.M., Scott, J.D., McGuinness, C.B., Carr, K.E., 1996. Early intestinal microparticle uptake in the rat. *J. Anat.* 189, 265–271.
- Hillyer, J.F., Albrecht, R.M., 2001. Gastrointestinal persorption and tissue distribution of differently sized colloidal gold nanoparticles. *J. Pharm. Sci.* 90 (12), 1927–1936.
- Hitosumatsu, O., Hamada, H., Naganuma, M., Inoue, N., Ishii, H., Hibi, T., Istikawa, H., 2005. Identification and characterisation of novel gut-associated lymphoid tissues in rat small intestine. *J. Gastroenterol.* 40, 956–963.
- Hodges, G.M., Carr, E.A., Hazzard, R.A., Carr, K.E., 1995. Uptake and translocation of microparticles in small intestine. Morphology and quantification of particle distribution. *Dig. Dis. Sci.* 40, 967–975.
- Hoshi, H., Horie, K., Tanaka, K., Nagata, H., Aizawa, S., Hiramoto, M., Ryouke, T., Aijima, H., 2001. Patterns of age dependant changes in the numbers of lymph follicles and germinal centres in somatic and mesenteric lymph nodes in growing C57Bl/6 mice. *J. Anat.* 198, 189–205.
- Jani, P.U., McCarthy, D.E., Florence, A.T., 1992. Nanosphere and microsphere uptake via Peyer's patches: observation of the rate of uptake in the rat after a single oral dose. *Int. J. Pharm.* 86, 239–246.
- Jenkins, P.G., Howard, K.A., Blackhall, N.W., Thomas, N.W., Davis, S.S., O'Hagan, D.T., 1994. Microparticulate absorption from the rat intestine. *J. Control. Rel.* 29, 339–350.
- Jepson, M.A., Collares-Buzato, C.B., Clark, M.A., Hirst, B.H., Simmons, N.L., 1995. Rapid disruption of epithelial barrier function by *Salmonella typhimurium* is associated with structural modification of intercellular junctions. *Infect. Immun.* 63, 356–359.
- Koudela, B., Modry, D., Svobody, M., Votycka, J., Vavra, J., Hudcovic, T., 1999. The severe combined immunodeficient mouse as a definitive host for *Sarcocystis muris*. *Parasitol. Res.* 85, 737–742.
- Leazer, T.M., Liu, Y., Klaassen, C.D., 2002. Cadmium absorption and its relationship to divalent metal transporter-1 in the pregnant rat. *Toxicol. Appl. Pharmacol.* 185, 18–24.
- LeFevre, M.E., Joel, D.D., Schidlovsky, G., 1985. Retention of ingested latex particles in Peyer's patches of germfree and conventional mice. *Proc. Soc. Exp. Biol. Med.* 179, 522–528.
- Limpanussorn, J., Simon, L., Dayan, A.D., 1998. Intestinal uptake of particulate material by dexamethasone-treated rats: use of a novel technique to avoid intestinal mucosal contamination. *J. Pharm. Pharmacol.* 50, 745–751.
- McClean, S., Prosser, E., Meehan, E., O'Malley, D., Clarke, N., Ramtoola, Z., Brayden, D., 1998. Binding and uptake of biodegradable poly-DL-lactide micro- and nanoparticles in intestinal epithelia. *Eur. J. Pharm. Sci.* 6, 153–163.
- McMinn, L., Hodges, G.M., Carr, K.E., 1996. Gastrointestinal uptake and translocation of microparticles in the streptozotocindabetic rat. *J. Anat.* 189, 553–559.
- Mandell, K.J., Babbin, B.A., Nusrat, A., Parkos, C.A., 2005. Junctional adhesion molecule 1 regulates epithelial cell morphology through effects on beta1 integrins and Rap1 activity. *J. Biol. Chem.* 280, 11665–11674.
- Martin-Padura, I., Lostaglio, S., Schneemann, M., Williams, L., Romano, M., Fruscella, P., Panzeri, C., Stoppacciaro, A., Ruco, L., Villa, A., Simmons, D., Dejana, E., 1998. Junctional adhesion molecule, a novel member of the immunoglobulin superfamily that distributes at intercellular junctions and modulates monocyte transmigration. *J. Cell Biol.* 142, 117–127.
- Mead, J.R., Arrowood, M.J., Healey, M.C., Sidwell, R.W., 1991. Chronic *Cryptosporidium parvum* infections in congenitally immunodeficient SCID and nude mice. *J. Infect. Dis.* 163, 1297–1304.
- Moghaddami, M., Cummins, A., Mayrhofer, G., 1998. Lymphocyte-filled villi: comparison with other lymphoid aggregations in the mucosa in the human small intestine. *Gastroenterology* 115, 1588–1591.
- Moyes, S.M., Smyth, S.H., Shipman, A., Long, S., Morris, J.F., Carr, K.E., 2007. Parameters influencing intestinal epithelial permeability and microparticle uptake in vitro. *Int. J. Pharm.* 337, 133–141.
- Mutwiri, G.K., Kosecka, U., Benjamin, M., Rosendal, S., Perdue, M., Butler, D.G., 2001. Mycobacterium avium subspecies paratuberculosis triggers intestinal pathophysiologic changes in beige/scid mice. *Comp. Med.* 51, 538–544.
- Naliboff, B.D., Mayer, M., Fass, R., Fitzgerald, L.Z., Chang, L., Bolus, R., Mayer, E.A., 2004. The effect of life stress on symptoms of heartburn. *Psychosom. Med.* 66, 426–434.
- Ohsugi, T., Kiuchi, Y., Shimoda, K., Oguri, S., Maejima, K., 1996. Translocation of bacteria from the gastrointestinal tract in immunodeficient mice. *Lab. Anim.* 30, 46–50.
- Ravi Kumar, M.N., 2000. Nano and microparticles as controlled drug delivery devices. *Pharm. Pharm. Sci.* 3 (2), 234–258.
- Riepenhoff-Talty, M., Uhnno, I., Chegas, P., Ogra, P.L., 1989. Effect of nutritional deprivation on mucosal viral infections. *Immunol. Invest.* 18, 127–139.
- Sababi, M., Bengtsson, U.H., 2001. Enhanced intestinal motility influences absorption in anaesthetized rat. *Acta Physiol. Scand.* 172, 115–122.
- Sharma, R., Schumacher, U., 2001. Carbohydrate expression in the intestinal mucosa. *Adv. Anat. Embryol. Cell Biol.* 160, 1–91.
- Sharma, R., Schumacher, U., Ronaasen, V., Coates, M., 1995. Rat intestinal mucosal responses to a microbial flora and different diets. *Gut* 36, 209–214.
- Sharma, R., van Damme, E.J.M., Peumans, W.J., Sarsfield, P., Schumacher, U., 1996. Lectin binding reveals divergent carbohydrate expression in human and mouse Peyer's patches. *Histochem. Cell Biol.* 105, 459–465.
- Smyth, S.H., Doyle-McCullough, M., Cox, O.T., Carr, K.E., 2005. Effect of reproductive status on uptake of latex microparticles in rat small intestine. *Life Sci.* 77, 3287–3305.
- Thomas, N.W., Jenkins, P.G., Howard, K.A., Smith, M.W., Lavelle, E.C., Holland, J., Davis, S.S., 1996. Particle uptake and translocation across epithelial membranes. *J. Anat.* 189, 487–490.
- Umemiya, R., Fukuda, M., Fujisaki, K., Matsui, T., 2005. Electron microscopic observation of the invasion process of *Cryptosporidium parvum* in severe combined immunodeficiency mice. *J. Parasitol.* 91, 1034–1039.
- Volkheimer, G., Schulz, F.H., Aurich, I., Strauch, S., Beuthin, K., Wendlandt, H., 1968. Persorption of particles. *Digestion* 1, 78–80.